CHINESE JOURNAL OF PHYSICS VOL. 52, NO. 2 April 2014

# Dynamics of Analytical Matter-Wave Solutions in One-Dimensional Bose-Einstein Condensates with Two- and Three-Body Interactions

Hai-Qin Jin,[1,2,*] Jun-Rong He,[2] Bin Xu,[3] and Ze-Bin Cai[4]

[1]*School of Physics and Mechanical & Electrical Engineering, Hubei University of Education, Wuhan 430205, China*

[2]*School of Physics, Huazhong University of Science and Technology, Wuhan 430074, China*

[3]*Department of Mathematics and Information Sciences, North China Institute of Water Conservancy and Hydroelectric Power, Zhengzhou 450011, China*

[4]*Scientific Research Department, Air Force Early Warning Academy, Wuhan 430019, China*

(Received July 30, 2013; Revised December 22, 2013)

Using the F-expansion method, we present analytical matter-wave solutions to Bose-Einstein condensates with two- and three-body interactions through the generalized one-dimensional Gross-Pitaevskii equation with time-dependent coefficients, for the experimentally relevant quadratic potential strength. Various shapes of the analytical matter-wave solutions which have important applications of physical interest are studied in detail. In particular, the matter-wave solitons are obtained in the quintic Gross-Pitaevskii equation model, which may be produced by tuning the cubic nonlinearity to zero via the Feschbach resonance technique. Direct numerical simulation has been performed to show the stable region of the matter-wave soliton.

DOI: 10.6122/CJP.52.780 PACS numbers: 05.45.Yv, 03.75.Lm

## I. INTRODUCTION

The Gross-Pitaevskii equation (GPE) and its variants are the most useful physical models in Bose-Einstein condensates (BECs), where it describes the behavior of the condensate wave function [1]. Various types of solutions to the GPE have been found to be of great interest due to their applications in physical systems, such as bright (dark) solitons [2], periodic traveling waves [3], and localized waves [4, 5]. In general, the GPE is a three space and one time dimensional nonlinear evolution equation, and is not integrable. When the transverse linear oscillator length is much smaller than the longitudinal length, the three-dimensional GPE can be reduced to a quasi-one-dimensional equation, which admits bright and dark solitons. Further, there has been an increased interest during recent times in studying the properties of BECs with time varying control parameters, especially for certain time-dependent atomic scattering lengths (nonlinearity) with time-independent harmonic potentials [6, 7].

Nonlinear interactions in BECs are usually of a cubic nature, but there are systems which engender cubic and quintic (CQ) nonlinearities, when the two- and three-body inter-

*Electronic address: hust316@126.com

 

actions are considered [8]. Furthermore, if the interaction of the atomic cloud are considered as well, the governing equation should still include the gain (loss) term. Most properties of the BECs are significantly affected by the interatomic interaction characterized by the s-wave scattering length, which is controlled by the Feschbach resonance (FR) technique [9].

Based on the above discussion, in this paper we will construct analytical matter-wave solutions of the CQ-GPE with quadratic potential and gain (loss) term. According to the zero-temperature mean-field theory, the dynamics of the one-dimensional BEC with two- and three-body interactions satisfies the following dimensionless GP equation [10]:

$$i\psi_t = -\frac{1}{2}\psi_{xx} + \alpha(t)x^2\psi + g(t)|\psi|^2\psi + \chi(t)|\psi|^4\psi + i\gamma(t)\psi, \tag{1}$$

where $\psi(x,t)$ is the normalized wave function of the condensate, with $N = \int |\psi|^2 \mathrm{d}x$ being the number of atoms. Here $t$ is the time measured in units of $1/\omega_\perp$, and $x$ is the position coordinate measured in units of $a_\perp$, where $\omega_\perp$ is the transverse trapping frequency, and $a_\perp$ is the linear oscillator lengths in the transverse direction. The functions $g(t)$ and $\chi(t)$ are the nonlinear coefficients corresponding to the two- and three-body interactions, respectively. In the experimental and theoretical studies [11–13], the real part of the three-body interaction term [$\chi(t)$ may be complex] can be $10^3 \sim 10^4$ times larger than the imaginary part, thus we may consider only the real quintic nonlinear regime [13]. $V(x) = x^2$ is the harmonic potential with $\alpha(t)$ being the strength varying with time $t$ [14]. The function $\gamma(t)$ is the gain or loss coefficient, which is phenomenologically incorporated to account for the interaction of atomic or thermal clouds in BECs.

In recent years, the CQ model has been intensively studied in the literature. For instance, the CQGPE in one-dimensions has been used to study the modulational instability [15], the energy-band structure and stability [13], and the matter-wave solutions in BECs [16]. Recently, analytical spatiotemporal periodic traveling wave and soliton solutions to the three-dimensional CQ nonlinear Schrödinger equation (NLSE) with distributed coefficients has been reported in [17]. If the quintic nonlinearity $\chi(t) = 0$, Eq. (1) degenerates to the standard GPE, which has been studied in Ref. [18]. The most interesting feature is that the cubic nonlinearity coefficient $g(t)$ can vanish in many nonlinear systems, which results in the quintic nonlinear Schrödinger equation (QNLSE). In BECs, the QNLSE can be derived by setting the s-wave scattering length $a_s(t)$ to zero via the FR technique [10, 19]. It is noted that the analytical matter-wave soliton solutions obtained in this paper are generally corresponding to the QNLSE. The QNLSE also appears in some NLSE-type systems when they near the transition from supercritical to subcritical bifurcations [20], pattern formation [21], and dissipative solitons [22].

The paper is organized as follows: in Sec. II, the solution method is presented. In Sec. III, some traveling matter-wave and soliton solutions are obtained. In this case, the cubic nonlinearity coefficient $g(t)$ is vanishing and Eq. (1) degenerates to the QNLSE. From the above mentioned facts, these matter-wave solitons may be generated by setting the s-wave scattering length $a_s(t)$ to zero via the FR technique. In addition, direct numerical simulation has been performed to show the stable region of the matter-wave soliton. Finally, the main findings are summarized in Sec. IV.

## II. SOLUTION METHOD

Utilizing the F-expansion technique and the balance principle [23], we write the complex wave function $\psi$ in terms of its amplitude and phase:

$$\psi(x,t) = A(x,t)\exp\left[iB(x,t)\right], \tag{2}$$

Substituting $\psi$ into Eq. (1), one arrives the following coupled equations:

$$A_t + A_x B_x + \frac{1}{2}AB_{xx} = \gamma A, \tag{3}$$

$$-AB_t + \frac{1}{2}(A_{xx} - AB_x^2) - \alpha x^2 A - gA^3 - \chi A^5 = 0. \tag{4}$$

We assume $A$ and $B$ to be of the form

$$A = f(t)\sqrt{F(\theta)} + h(t)\sqrt{F^{-1}(\theta)}, \tag{5}$$

$$\theta = k(t)x + \omega(t), \tag{6}$$

$$B = a(t)x^2 + b(t)x + e(t), \tag{7}$$

where $f, h, k, \omega, a, b, e$ are real functions of $t$ to be determined, and $F$ is a Jacobi elliptic function (JEF), which in general satisfies the following general first and second-order nonlinear ordinary differential equations: $(\frac{\mathrm{d}F}{\mathrm{d}\theta})^2 = c_0 + c_2F^2 + c_4F^4$, and $\frac{\mathrm{d}^2F}{\mathrm{d}\theta^2} = c_2F + 2c_4F^3$, where $c_0, c_2$, and $c_4$ are real constants related to the elliptic modulus $M$ of the JEFs (see Table I).

Substituting Eqs. (5)–(7) into Eqs. (3) and (4) and requiring that $x^jF^{\pm n/2}, (j = 0, 1, 2; n = 0, 1, 2, 3, 4, 5)$, and $\sqrt{c_0 + c_2F^2 + c_4F^4}$ of each term be separately equal to zero, we obtain a system of ordinary differential equations (ODEs) for the parameter functions:

$$\frac{\mathrm{d}\Omega_i}{\mathrm{d}t} + a\Omega_i - \gamma\Omega_i = 0, \tag{8}$$

$$\frac{\mathrm{d}k}{\mathrm{d}t} + 2ka = 0, \tag{9}$$

$$\frac{\mathrm{d}\omega}{\mathrm{d}t} + bk = 0, \tag{10}$$

$$\frac{\mathrm{d}a}{\mathrm{d}t} + 2a^2 + \alpha = 0, \tag{11}$$

TABLE I: Jacobi elliptic functions.

| | $c_0$ | $c_2$ | $c_4$ | $F$ | $M=0$ | $M=1$ |
|---|---|---|---|---|---|---|
| 1 | 1 | $-(1+M^2)$ | $M^2$ | sn | sin | tanh |
| 2 | $1-M^2$ | $2M^2-1$ | $-M^2$ | cn | cos | sech |
| 3 | $M^2-1$ | $2-M^2$ | $-1$ | dn | 1 | sech |
| 4 | $M^2$ | $-(1+M^2)$ | 1 | ns | csc | coth |
| 5 | $-M^2$ | $2M^2-1$ | $1-M^2$ | nc | sec | cosh |
| 6 | $-1$ | $2-M^2$ | $M^2-1$ | nd | 1 | cosh |
| 7 | 1 | $2-M^2$ | $1-M^2$ | sc | tan | sinh |
| 8 | $1-M^2$ | $2-M^2$ | 1 | cs | cot | csch |
| 9 | 1 | $-(1+M^2)$ | $M^2$ | cd | cos | 1 |
| 10 | $M^2$ | $-(1+M^2)$ | 1 | dc | sec | 1 |

$$\frac{\mathrm{d}b}{\mathrm{d}t}+2ab=0, \tag{12}$$

$$f\left(\frac{3}{8}k^2c_4-\chi f^4\right)=0, \tag{13}$$

$$h\left(\frac{3}{8}k^2c_0-\chi h^4\right)=0, \tag{14}$$

$$\frac{\mathrm{d}e}{\mathrm{d}t}+\frac{1}{2}b^2-\frac{1}{8}k^2c_2+3gfh+10\chi f^2h^2=0, \tag{15}$$

$$gf^3+\frac{1}{8}hk^2c_4+5\chi f^4h=0, \tag{16}$$

$$gh^3+\frac{1}{8}fk^2c_0+5\chi fh^4=0, \tag{17}$$

where $\Omega_i=f,h$.

Defining a single auxiliary function $\delta(t)=\int_0^t a\mathrm{d}t$, we obtain the following solutions by solving the ODEs (8)–(17):

$$S=S_0\exp\left(-2\delta\right), \tag{18}$$

$$f = f_0 \exp(-\delta) \exp\left(\int_0^t \gamma \mathrm{d}t\right), \quad h = \epsilon \left(\frac{c_0}{c_4}\right)^{\frac{1}{4}} f, \tag{19}$$

$$\omega = \omega_0 - b_0 k_0 \int_0^t \exp(-4\delta)\mathrm{d}t, \tag{20}$$

$$e = e_0 + \frac{1}{8}\left[\left(c_2 + 18\epsilon^2\sqrt{c_0 c_4}\right) k_0^2 - 4b_0^2\right] \int_0^t \exp(-4\delta)\mathrm{d}t, \tag{21}$$

where $S \equiv S(t) = k, b$. The subscript "0" denotes the value of the given function at $t = 0$. The parameter $\epsilon$ can take the values $0, \pm 1$. Then the nonlinearity coefficients $g(t)$ and $\chi(t)$ are given by

$$g = -\frac{2c_4}{f_0^2} k_0^2 \epsilon (\frac{c_0}{c_4})^{\frac{1}{4}} \exp(-2\delta) \exp(-2\int_0^t \gamma \mathrm{d}t), \tag{22}$$

$$\chi = \frac{3c_4}{8f_0^4} k_0^2 \exp(-4\int_0^t \gamma \mathrm{d}t), \tag{23}$$

The parameter $\alpha(t)$ is implicit in $\delta(t)$ via Eq. (18).

Recombining Eqs. (11) and (22), we obtain

$$-\frac{g_{tt}}{2g} - \frac{g_t^2}{g^2} + \frac{2\gamma g_t}{g} - \gamma_t + 2\gamma^2 + \alpha = 0, \tag{24}$$

Eqs. (23) and (24) can be understood as the so-called integrability conditions in the present paper.

Finally, the analytical matter-wave solutions of Eq. (1) are given by

$$\psi = f_0 \exp(-\delta) \exp\left(\int_0^t \gamma \mathrm{d}t\right) \left[\sqrt{F(\theta)} + \epsilon \left(\frac{c_0}{c_4}\right)^{\frac{1}{4}} \sqrt{F^{-1}(\theta)}\right] \times \exp\left[i(ax^2 + bx + e)\right]. \tag{25}$$

Therefore, as long as one chooses the constants according to the relations listed in Table I and substitutes the appropriate $F(\theta)$ into Eq. (25), one obtains the analytical matter-wave solutions to Eq. (1). When $0 < M < 1$, the JEFs are periodic traveling wave solutions. When $M \to 0$, the periodic traveling wave solutions evolve into the periodic trigonometric functions. When $M \to 1$, the periodic traveling wave solutions become time-dependent soliton solutions. When $M = 0$ or 1, only some of the functions may be utilized, because of singularities developing.

From Eqs. (18)–(21) one can see that the analytical solution of Eq. (1) can be found only if Eq. (11) for the chirp function $a(t)$ can be solved. The solutions for all other equations explicitly or implicitly depend on $a$; the equation for $a$ is a Riccati-type equation.

Interestingly, Eq. (11) can be expressed as a Schrödinger eigenvalue problem via a change of variable, $a(t) = \frac{1}{2}\frac{\mathrm{d}\ln[\varphi(t)]}{\mathrm{d}t}$:

$$\varphi_{tt} + 2\alpha\varphi = 0, \tag{26}$$

Taking advantage of this connection, below we show that, corresponding to some solvable quantum-mechanical and physical systems, one can identify the soliton configurations. Although a host of time-dependent oscillator frequencies can be addressed, we will only demonstrate in the text an experimentally realizable example.

Considering that some physical experiments are expected to create solitary waves [24, 25], in the following we take $\alpha(t) = -\Omega_0^2/2$ with $\Omega_0 \approx 0.1$. With this we get the variable $\varphi(t) = c_1 e^{\Omega_0 t} + c_2 e^{-\Omega_0 t}$, where $c_1$ and $c_2$ are real constants. As an example, we choose $c_1 = c_2 = 1/2$ in this paper, but many other values can be selected as well. For this, the chirp function $a(t) = \Omega_0 \tanh(\Omega_0 t)/2$ and thus the auxiliary function $\delta(t) = \ln[\cosh(\Omega_0 t)]/2$. When these parameters are calculated, exact solutions of Eqs. (18)–(23) can be obtained if one has chosen the gain (loss) function $\gamma(t)$ specifically. Next, we will study the dynamics and possible physical applications of the analytical traveling matter-wave and soliton solutions of Eq. (1) in the above displayed parameters for different choices of $\gamma(t)$.

## III. ANALYTICAL TRAVELING MATTER-WAVE AND SOLITON SOLUTIONS

When $0 < M < 1$, the periodic traveling matter-wave solutions to Eq. (1) can be found. From Eq. (23) one can see that the sign of the quintic interaction $\chi(t)$ depends on $c_4$ appearing in Table I. When $c_4 > 0$, the three-body interaction is repulsive; otherwise the three-body interaction is attractive. As can be seen from Table I, F = cn and dn correspond to the attractive three-body interactions, the other cases correspond to repulsive three-body interactions. Furthermore, if $\epsilon \neq 0$, we find that the sign of the cubic interaction $g(t)$ is opposite to that of $c_4$ according to Eq. (22), i.e., $c_4 > 0$ denotes the attractive two-body interactions, $c_4 < 0$ denoting the repulsive two-body interactions. Hence, attractive two-body interaction and repulsive three-body interaction, and repulsive two-body interaction and attractive three-body interaction may provide traveling matter waves in BECs. If $\epsilon = 0$, only the three-body interaction is available. In this case, the corresponding traveling matter waves may be generated by setting the s-wave scattering length $a_s(t)$ to zero via the FR technique. Some typical examples of traveling matter waves are shown in Figs. 1 and 2, corresponding to $b_0 = 0$ and $b_0 \neq 0$, respectively.

In the following, we mainly focus on the soliton solutions by taking the elliptic modulus $M$ as 1. According to the conditions of Eqs. (21), (22), and (25), $c_0$ and $c_4$ take the same sign. After some analysis, we find that only the first three lines in Table I are able to give out soliton solutions. In the first line of Table I, because $c_0 \neq 0$, one takes $\epsilon = 0$ to avoid a possible divergence caused by $1/F(\theta)$ in the second term of $A(x,t)$. As a consequence, the cubic nonlinearity $g(t) = 0$, and a tanh form soliton solution can be obtained. This case corresponds to the repulsive three-body interaction. In the second and third lines, because

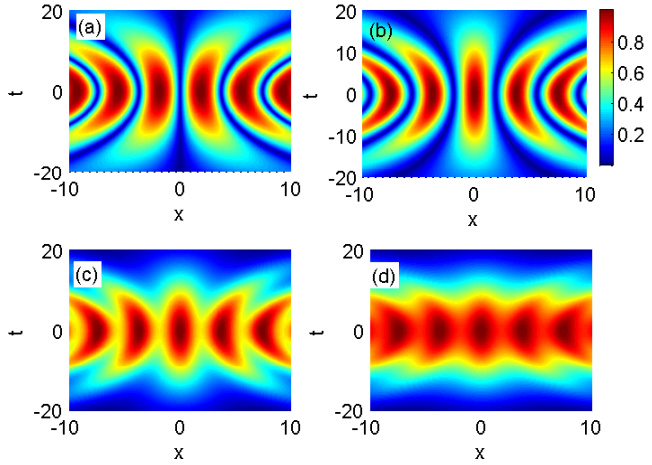


FIG. 1: Periodic traveling wave solutions in terms of JEFs to Eq. (1). (a) Intensity $|\psi|^2$ for (a) $F = \mathrm{sn}$, (b) $F = \mathrm{cn}$, and (c) and (d) $F = \mathrm{dn}$, presented as functions of $x$ and $t$. For (a)–(c) $\epsilon = 0$, $M = 0.5$, for (d) $\epsilon = 1$, $M = 0.99$. Other coefficients are: $\gamma = \gamma_0 = 0$, $f_0 = k_0 = 1$, $\omega_0 = b_0 = e_0 = 0$.

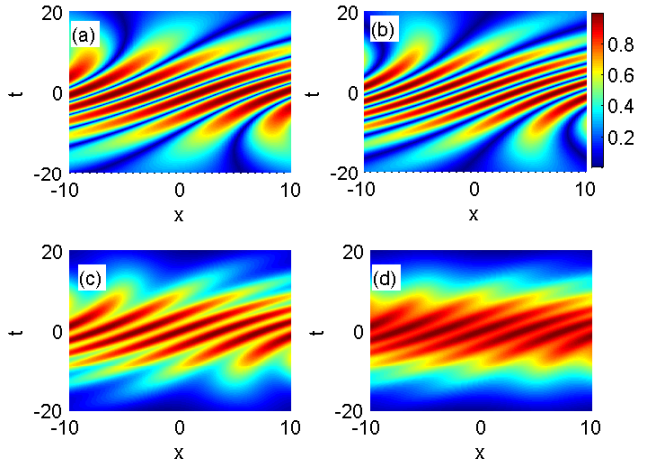


FIG. 2: (a) The same as in Fig. 1 except for $b_0 = 1$.

$c_0$ is zero, the value of $g(t)$ is zero according to the condition of Eq. (22), and a bright soliton solution is obtained. In this case, the three-body interaction is attractive. Thus, for these two classes of soliton solutions, only Eq. (23) survives, and the cubic nonlinearity is

zero. After these parameters are given, the bright and dark soliton solutions are

$$\psi_B = f_0 \exp(-\delta) \exp\left(\int_0^t \gamma \mathrm{d}t\right) \sqrt{\mathrm{sech}(\theta)} \times \exp\left[i(ax^2 + bx + e)\right]. \tag{27}$$

and

$$\psi_D = f_0 \exp(-\delta) \exp\left(\int_0^t \gamma \mathrm{d}t\right) \sqrt{\tanh(\theta)} \times \exp\left[i(ax^2 + bx + e)\right]. \tag{28}$$

where the functions $\delta$, $\theta$, and $b$ are given above.

First, we consider the case of $\gamma = \gamma_0 = 0$. From Eq. (23), one obtains that the quintic interaction coefficient $\chi(t)$ is a constant. The corresponding bright and dark soliton solutions can be obtained from Eqs. (27) and (28). The spatiotemporal evolution of the wave is shown in Fig. 3. Figures 3(a) and 3(b) describe the density profiles of the wave function $\psi$ for the bright and dark one with $b_0 = 0$, respectively. Figures 3(c) and 3(d) describe the contour plots corresponding to Figs. 3(a) and 3(b). At the beginning, the solitons start with low amplitude and large width. After some time, their amplitudes become high but their widths become small; as time goes on their amplitudes decrease and the widths increase gradually. This can be clearly seen from the behavior of their amplitudes and widths. The amplitude of the soliton is proportional to $\sqrt{\mathrm{sech}(\Omega_0 t)}$ while the width of the soliton is proportional to $1/\mathrm{sech}(\Omega_0 t)$. So the amplitude and width of the soliton depend on the strength of the harmonic trap, which may be adjusted by the magnetic field. Figure 3 may correspond to a physical experiment where a BE condensate lasts only for a limited time interval.

Next, we consider $\gamma = \gamma_0 = -0.01$. In this case, the quintic interaction coefficient $\chi(t) = \frac{3c_4}{8f_0^4} k_0^2 \exp(-4\gamma_0 t)$. The analytical matter-wave soliton solutions corresponding to Eq. (1) are shown in Fig. 4. Figures 4(a) and 4(b) describe the density profiles of the wave function $\psi$ for the bright and dark one with $b_0 = 0$, respectively. Figures 4(c) and 4(d) describe the contour plots corresponding to Figs. 4(a) and 4(b). The amplitude of the soliton is proportional to $\sqrt{\mathrm{sech}(\Omega_0 t)} e^{\gamma_0 t}$, while the width of the soliton is in the same form as the case $\gamma_0 = 0$. However, unlike in Fig. 3, these solitons start from a much larger width but with smaller value when they attenuate, which is caused by the term $\exp(-4\gamma_0 t)$. This indicates that the larger the interaction of atomic or thermal clouds in BECs, the larger the attenuation of the condensate. Moreover, the three-body interatomic interaction $\chi(t)$ depends on the the gain or loss term $\gamma$, which implies that $\chi(t)$ accounts for the interaction of the condensation with the thermal cloud.

A physically interesting case can be observed by choosing the gain (loss) term as $\gamma = \cos(t)$. For this choice, we have $\chi(t) = \frac{3c_4}{8f_0^4} k_0^2 \exp\left[-4\sin(t)\right]$, which varies periodically with time. The analytical matter-wave soliton solutions corresponding to Eq. (1) are shown in 5. Figures 5(a) and 5(b) describe the density profiles of the wave function $\psi$ for the bright and dark ones with $b_0 = 0$, respectively. Figures 5(c) and 5(d) describe the contour plots corresponding to Figs. 5(a) and 5(b). It is seen that the solitons exhibit the collapse and revival behavior during the propagation. The amplitude of the soliton is proportional to

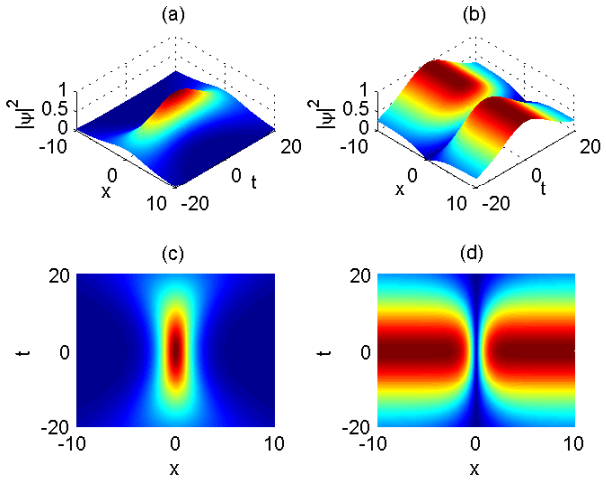


FIG. 3: Soliton solutions to Eq. (1) as functions of time. Intensity $|\psi|^2$ for (a) bright soliton ($F$ = sech), and (b) dark soliton ($F$ = tanh) presented as functions of $x$ and $t$. (c) and (d) are the contour plots of densities for (a) and (b), respectively. Coefficients and parameters are $\gamma = \gamma_0 = 0,\ M = f_0 = k_0 = 1,\ \epsilon = \omega_0 = b_0 = e_0 = 0$.

$\sqrt{\text{sech}(\Omega_0 t)}e^{\sin(t)}$ while the width of the soliton is proportional to $1/\text{sech}(\Omega_0 t)$. The collapse and revival of the atomic condensate and the amplification through the periodic exchange of atoms with the background is obviously due to the sinusoidal nature of the gain function. This fact may be amenable for verifying the experiments carried out in [24, 26]. In view of the nontrivial nature of the phase and its connection with the soliton profile, the nature of the spatiotemporal dynamics of the obtained matter-wave solitons are worth discussing. The quadratic nature of the phase with respect to the space coordinate is shown in Figs. 5(e) and 5(f). It is observed that the wave trains show $\pi$ jumps at the time boundary $t = 0$.

We did not investigate the case of $b_0 \neq 0$, since this only leads to the soliton moving with respect to time. It is pointed out that the matter-wave soliton solutions found here, as previously referred, may be realized in BECs by tuning the cubic nonlinearity $g(t)$ to zero using the FR technique.

To demonstrate the stability of the solutions, we performed direct numerical simulations of the matter-wave soliton for Eq. (1), with initial data coming from Eq. (27). We utilized the split-step Fourier-transform method to run simulations of the wave-evolution. The domain was composed of $N = 512$ grid points and the step size of the time integration was $\Delta t = 0.005$. An example of such behavior is displayed in Fig. 6, which essentially presents a numerical recap of Fig. 3(a). Here the time is $t \in [0, 80]$, but similar behavior occurs in the interval $t \in [-80, 0]$ because of the symmetry of the solution. Our numerical simulation shows that the soliton presents a nearly stable state at $t \in [-20, 20]$ while it is unstable out of this region. This may make the observation of BEC more likely in the experiment when it is performed during the condensate time interval. For example, when considering the radial frequency $\omega_\perp = 2\pi \times 700$ Hz of a $^7$Li condensate, the unit of time is

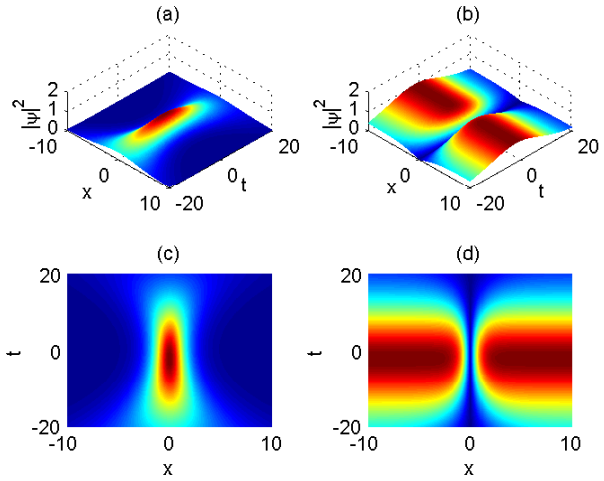


FIG. 4: Soliton solutions to Eq. (1) as functions of time. Intensity $|\psi|^2$ for (a) bright soliton ($F = \text{sech}$), and (b) dark soliton ($F = \tanh$) presented as functions of $x$ and $t$. (c) and (d) are the contour plots of the densities for (a) and (b), respectively. Other parameters are the same as in Fig. 3, except for $\gamma = -0.01$.

0.225 ms, which means that our condensate in Fig. 6 may be stable in experiments for no more than 4.5 ms.

## IV. CONCLUSIONS

Using the F-expansion method we have constructed analytical matter-wave solutions for BECs with two- and three-body interactions through the one-dimensional GPE with time-dependent coefficients. In particular, some matter-wave solitons are obtained in the QNLSE model, which may be generated by tuning the cubic nonlinearity to zero via the FR technique. Finally, direct numerical simulation has been performed to show the stable region of the matter-wave soliton.

## Acknowledgements

This work is supported by the National Natural Science Foundation of China under Grant No. 11105057, the foundation of Hubei University of Education under Grant No. 2009B013, and the Project of Excellent Teacher Team of Hubei University of Education Under Grant No. 2012KB302.

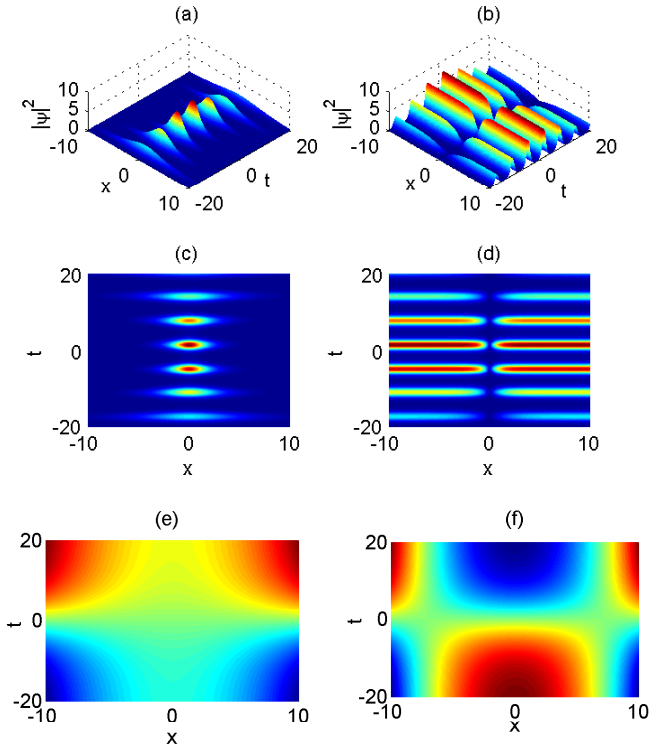


FIG. 5: Soliton solutions to Eq. (1) as functions of time and the corresponding phase distributions. Intensity $|\psi|^2$ for (a) bright soliton ($F$ = sech), and (b) dark soliton ($F$ = tanh) presented as functions of $x$ and $t$. (c) and (d) are the contour plots of the densities for (a) and (b), respectively. (e) and (f) are the phase distributions for (a) and (b), respectively. Other parameters are the same as in Fig. 3, except for $\gamma = \cos(t)$.

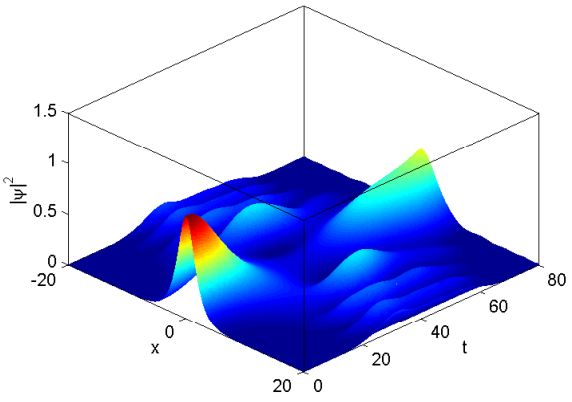


FIG. 6: Direct numerical simulation of a BE condensate. The solution is chosen from Fig. 3(a) with initial values given by Eq. (27). The parameter values are the same as in Fig. 3(a).

## References


[1] L. P. Pitaevskii and S. Stringari, *Bose-Einstein Condensation*, (Oxford University Press, Oxford, 2003).

[2] F. S. Cataliotti *et al.*, Science **293**, 843 (2001); K. E. Strecker, G. B. Partridge, A. G. Truscott, and R. G. Hulet, Nature (London) **417**, 150 (2002); U. Al Khawaja, H. T. C. Stoof, R. G. Hulet, K. E. Strecker, and G. B. Partridge, Phys. Rev. Lett. **89**, 200404 (2002).

[3] N. N. Akhmediev and A. A. Ankiewicz, *Solitons*, (Chapman and Hall, London, 1997); A. Hasegava and M. Matsumoto, *Optical Solitons in Fibers*, (Springer, New York, 2003); V. E. Zakharov and A. B. Shabat, Sov. Phys. JETP **34**, 62 (1972).

[4] J. Belmonte-Beitia, V. M. Pérez-García, V. Vekslerchik, and V. V. Konotop, Phys. Rev. Lett. **100**, 164102 (2008).

[5] J. Belmonte-Beitia and G. F. Calvo, Phys. Lett. A **373**, 448 (2009).

[6] U. A. Khawaja, J. Phys. A: Math. Gen. **39**, 9679 (2006).

[7] Z. X. Liang, Z. D. Zhang, and W. M. Liu, Phys. Rev. Lett. **94**, 050402 (2005); B. Li, X.-F. Zhang, Y.-Q. Li, Y. Chen, and W. M. Liu, Phys. Rev. A **78**, 023608 (2008); J.-K. Xue, J. Phys. B **38**, 3841 (2005).

[8] F. K. Abdullaev and M. Salerno, Phys. Rev. A **72**, 033617 (2005).

[9] S. Inouye *et al.*, Nature **392**, 151 (1998); E. A. Donley *et al.*, Nature **412**, 295 (2001).

[10] F. Dalfovo, S. Giorgini, L. P. Pitaevskii, and S. Stringari, Rev. Mod. Phys. **71**, 463 (1999).

[11] A. E. Leanhardt *et al.*, Phys. Rev. Lett. **89**, 040401 (2002); T. Köhler, Phys. Rev. Lett. **89**, 210404 (2002); P. Pieri and G. C. Strinati, Phys. Rev. Lett. **91**, 030401 (2003); B. Laburthe Tolra *et al.*, Phys. Rev. Lett. **92**, 190401 (2004); J. Söding *et al.*, Appl. Phys. B: Laser Opt. **69**, 257 (1999).

[12] U. Roy, R. Atre, C. Sudheesh, C. N. Kumar, and P. K. Panigrahi, J. Phys. B **43**, 025003 (2010).

[13] A.-X. Zhang and J.-K. Xue, Phys. Rev. A **75**, 013624 (2007).

[14] Yu. Kagan, A. E. Muryshev, and G. V. Shlyapnikov, Phys. Rev. Lett. **81**, 933 (1998); J. J. G. Ripoll, and V. M. Pérez-García, Phys. Rev. A **59**, 2220 (1999); F. Kh. Abdullaev and R. Galimzyanov, J. Phys. B **36**, 1099 (2003); G. Theocharis1, Z. Rapti, P. G. Kevrekidis, D. J. Frantzeskakis1, and V. V. Konotop, Phys. Rev. A **67**, 063610 (2003).

[15] E. Wamba, A. Mohamadou, and T. C. Kofané, Phys. Rev. E **77**, 046216 (2008); J. Phys. B **41**, 225403 (2008).

[16] A. Mohamadou, E. Wamba, S. Y. Doka, T. B. Ekogo, and T. C. Kofane, Phys. Rev. A **84**, 023602 (2011); A. Mohamadou, E. Wamba, D. Lissouck, and T. C. Kofane, Phys. Rev. E **85**, 046605 (2012).

[17] H. Kumar, A. Malik, and F. Chand, J. Math. Phys. **53**, 103704 (2012).

[18] N. Z. Petrović, M. Belić, and W.-P. Zhong, Phys. Rev. E **81**, 016610 (2010); N. Z. Petrović, N. B. Aleksić, A. Al Bastami, and M. R. Belić, Phys. Rev. E. **83**, 036609 (2011); A. Al Bastami, M. R. Belić, D. Milović, and N. Z. Petrović, Phys. Rev. E. **84**, 016606 (2011).

[19] V. A. Brazhnyi, V. V. Konotop, and L. P. Pitaevskii, Phys. Rev. A **73**, 053601 (2006).

[20] E. A. Kuznetsov, J. Exp. Theor. Phys. **89**, 163 (1999); D. Agafontsev, F. Dias, and E. A. Kuznetsov, JETP Lett. **87**, 667 (2008).

[21] M. C. Cross and P. C. Hohenberg, Rev. Mod. Phys. **65**, 851 (1993).

[22] J. M. Soto-Crespo, N. Akhmediev, and A. Ankiewicz, Phys. Rev. Lett. **85**, 2937 (2000).

[23] M. Belić, N. Petrović, W. P. Zhong, R. H. Xie, and G. Chen, Phys. Rev. Lett. **101**, 123904 (2008).

[24] L. Khaykovich *et al.*, Science **296**, 1290 (2002).

[25] K. E. Strecker, G. B. Partridge, A. G. Truscott, and R. G. Hulet, New J. Phys. **5**, 73 (2003);

S. Rajendran, P. Muruganandam, and M. Lakshmanan, Physica D **239**, 366 (2010).
[26] K. E. Strecker *et al.*, Nature (London) **417**, 150 (2002); U. Al Khawaja *et al.*, Phys. Rev. Lett. **89**, 200404 (2002).